Semiconductor Optoelectronics, *Vol. 42 No. 1 (2023), 574-585*
https://bdtgd.cn/

Semiconductor Optoelectronics ISSN: 1001-5868

OPTIMIZATION AND SIMULATIION OF MECHANICAL PROPERTIES IN JOINING DISSIMILAR METALS BY FRICTION WELDED

Neeraja Pilli
Research scholar, Department of Mechanical Engineering, GIET University, Odissa, India
Email: neerunitw@gmail.com

Dr. Ajit Kumar Senapati
Professor, Department of Mechanical Engineering, GIET University, Odissa, India Email: senapati.ajit@gmail.com

Dr. Swarnalatha Moora
Head Laboratory, Department of Quality, Andhra University, Andhra Pradesh, India Email: Blessyracheal@gmail.com

Abstract
Significant advancements in industrial applications have led to the widespread use of friction welding (F.W.) in recent years (I.A.). F.W. is one of the most productive and inexpensive ways to connect dissimilar metals. Stainless steel (S.S.) and EN3B were submitted to F.W. testing within the confines of this study. Rotational speed, frictional time/pressure, and forging time/pressure were processing parameters. This study aims to raise the tensile strength of a composite made of two different metals by modifying the F.W. factors in such a way that they bring together stainless steel and tungsten carbide (T.S.). The material's T.S. was investigated in a series of studies with several configurations of the process conditions. It was found that the procedure was successful and that the strength of the welded connections varied with the settings of the process variables. The welds were tested using T.S. The results were documented in a table with the input variables. Once the hardness distribution was plotted, it was found that there was a hardness peak near the joint contact. The joint's microstructure was also characterized by observation.

KEYWORDS: *Friction Welding, Stainless Steel, EN3B, Tensile Strength, Micro-structural Analysis*

1. INTRODUCTION

FW is becoming increasingly common in I.A. as an extensive production process for attaching the parts, and it is applied frequently in various businesses. In industrial settings, machinery equipment is an essential factor. Welding is a typical procedure for introducing and using elements or substances (N. A. Kozyrev, 2015). The F.W. procedure is a solid-state welding technique wherein the surfaces of the materials being welded are rubbed with each other to generate heat and, as a result, give pressure for connecting two different types of materials while they are in a molten state, which ultimately results in a high-quality sample (Wibowo, Ismail, and Jamari 2016). There are two primary types of F.W., known as pressure welding and melt welding, respectively. The pressure welding process, known as friction welding, does not involve using any electric power source (Wibowo, Ismail, and Jamari 2016). Only friction between the surfaces of 2 materials generates mechanical energy, which is liable for the character's heat distribution and is used to weld. Our primary purpose is to conduct experimental research to combine two various types of metals, and our secondary objective is to increase the T.S. of the material by experimenting with different F.W. parameters.

2. LITERATURE REVIEW

1. In a study quite similar to the one that (Sahin 2005; Rafati et al. 2021) conducted, friction welding was performed on medium carbon steel (M.C.S.) and high-speed steel (H.S.S.). Such materials were put through the notch impact, fatigue, and T.S. tests. Test conducted on material when a constant tensile load gets superimposed by some fluctuating high tensile loads, known as fatigue tests, the pressure of 225MPa. The notch impact test can easily fracture the welded joints. High-speed steel has less notch impact toughness as compared to that welded parts.

2. P. ShenbagaVelu et al. [12], studied numerical analysis on a titanium joint made with friction welding. This project employs a titanium rod with a 10mm diameter and a 20mm length with ABAQUS software. This paper assumes an angular velocity of 108.3 rad/s and a pressure of 10 bars. The centre line of the weld is heated to 906oC for 3 seconds using a coupled field thermo-mechanical study. Away from the weld's middle line, the temperature dropped steadily, 020049-2 with time. The tensions are at their highest at a distance of 1.5 mm from the weld's centre line.
3. Palanivel et al. [13] investigated the parameters of friction welding on titanium tubes, first settling on tubes 60 mm in diameter and 4 mm in thickness. During the testing phase, they discovered weak welds and an imperfect welding zone at lower-than-expected levels of difficulty. They found that weld strength may be enhanced by using medium friction welding parameters, such as 2000 R.P.M. and 32 seconds of friction and a displacement of 2mm. This is because excessive parameters result in poor weld strength due to considerable heat created at the weld zone.
4. Friction welding was used by Takeshi Shinoda, et al. [14], to combine cast iron, another comparable material. It has focused mostly on tensile qualities against welding settings. It has been stated that fusion welding is not advised for cast iron or materials with comparable properties to prevent unnecessary preheating and postheating. In this operation, FC200 grey cast iron with dimensions of 25 mm in diameter and 140 mm in length is used, with a spindle speed of 2360 RPM and a forge pressure of 2200 MPa being taken into account. It was determined that a reduction in the rate of heat input led to an increase in tensile strength. Weld joint strength is comparable to the base material at low heat input rate and upset speed.
5. PandiaRajan et al. [15], focused on SA213 bar and SA 387 bar, two quite different materials. To link the bars together, tiny holes are drilled onto the outside surface of each one. The bars may be linked either with or without a hole. The hardness test was also done on the weld interface zone between the two specimens, and the results confirmed that the without-

hole specimen was stronger than the with-hole specimen. Additionally, it was shown that the hardness of the specimens was much improved after they were made hole-free

3. METHODOLOGY

3.1 Materials Used

Both SS, as well as mild steel (430 F and En3B), were involved in the carrying out of this investigation. Material selection or suitability for welding process is done on the basis of two parameters. These are: material strength and deformation capacity because of heat (B. Srinivas, 2018). To attain a good quality joint, materials must be strong enough to refrain from high axial pressure, and can exhibit high temperature or heat to undergo the process of welding. Chemical composition (CC) of S.S., EN3B as well as mild steel are provided in Table 1, Table 2 & Table 3 accordingly.

Table 1: CC of Stainless Steel

Material	Values	C	Mn	Cr	S	Si
Stainless Steel	Max	0.11	1.23	16.1-17.9	0.14	1
	Observed value	0.1	0.4	17.52	0.15	0.78
EN3B	Max	0.24	0.99	0.05	0.05	0.36
	Observed value	0.22	0.82	0.012	0.04	0.215
Mild Steel	Max	0.22	1.52	0.055	0.046	0.41
	Observed value	0.18	0.82	0.014	0.03	0.22

3.2 Specimen Geometry

Each specimen was a cylinder constructed of S.S. measuring 12 millimetres in diameter & 125 millimetres in length. The EN3B samples measured 15 millimetres in diameter & 75 millimetres in length(Shubhavardhan and Surendran 2012). Lathe work was done to get the cylindrical samples to a diameter of 12 millimetres.

3.3 Procedure

Direct drive friction welding setup with updated joint shape combines M.S. and SS 304. Weld specimens are measured at 12mm in diameter and 125mm in length, and 15mm in diameter and 75mm in length. Essentially, the whole experimental strategy is broken down into three distinct stages that make up the design of the procedure of the experiment. There are three stages: 1) preparation, 2) execution and 3) evaluation. Figure **shows the D.O.E. block diagram. Speed, friction time, forging time, pressure, and forging pressure are all critical process factors that may be adjusted in a friction welding operation. Table 3.1 lists the process's three stages, while Table 3.2 lists the trail's specifics—indeterminate factors such as component alignment, weld cleanliness, surface polish, etc. For the sake of the test, certain factors that can't be manipulated are tamed.

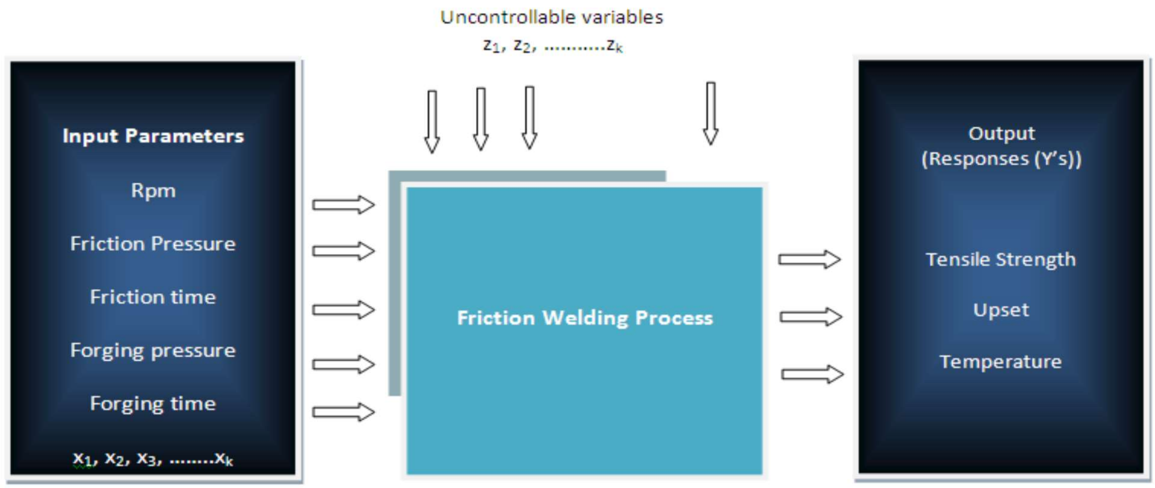

Figure 3.1 Block diagram of design of experiment

Table 3.1 Process Parameters of the Experiment

S.No	Welding Parameters	Low	Medium	High
1	R.P.M.	1400	1700	2000
2	Friction Pressure (MPa)	30	50	70
3	Friction Time (Seconds)	1	2	3
4	Forging Pressure (MPa)	100	120	140
5	Forging Time (Seconds)	2	4	6

The Linear Friction Welding (L.F.W.) principles were implemented in the planning and construction of the setup.

a)

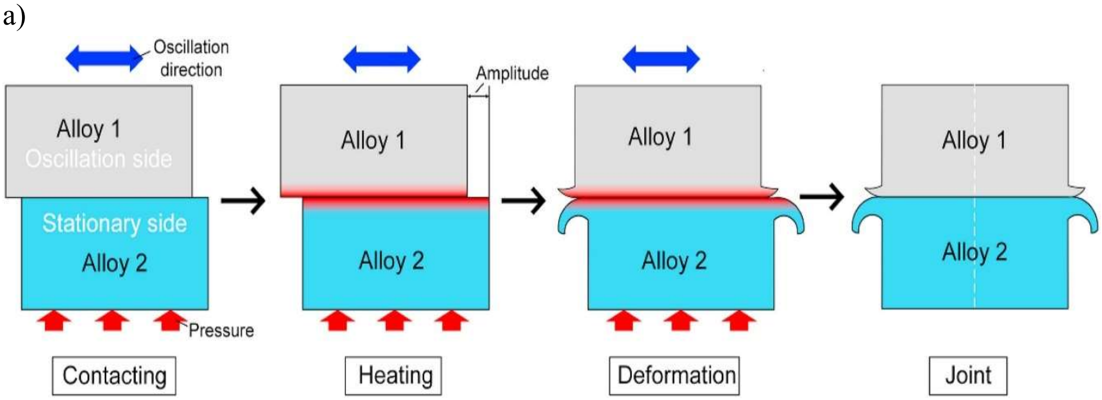

Figure 1: Friction Welding Trails

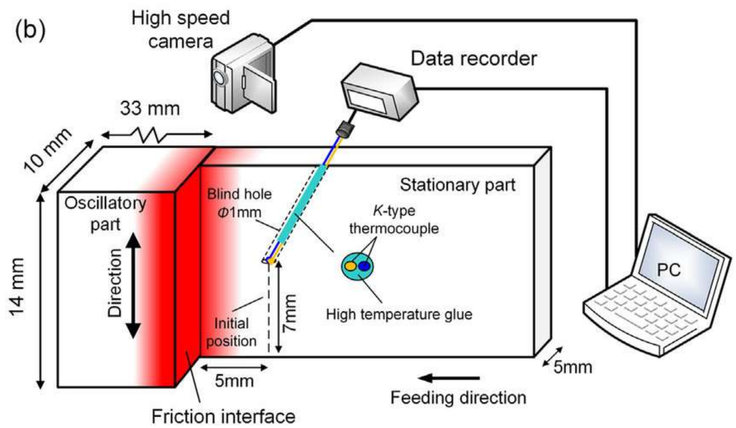

Figure 2: Linear friction welding setup

Prior to welding, acetone was used to clean the surfaces of the materials. Emery paper was utilized for sough grinding. It was determined that the F.W. machine F.W.G. 20/300-S was the most suitable option due to its high accuracy and great repeatability during the process. An A.C. motor was implemented so that the spindle could be operated. A load cell was used to measure friction & upset forces, and a computer ensured that they were managed in an accurate manner. All important data pertaining to each weld was properly collected(Karadge et al. 2008).

- Force of Friction
- "Burn-off length"
- Rotational Speed
- Upset Force

Table 2: Process Parameters at Different Levels

S. No.	Welding Input Parameters(X)	Level_1	Level_2	Level_3
1.	Rotation Speed(rpm)	1200	1500	1800
2.	FP(Friction Pressure)(MPa)	40	60	90
3.	FT(Friction Time)(s)	2	3	4
4.	FOP(Forging Pressure)(MPa)	80	100	120
5.	FOT(Forging Time)(s)	4	6	8

4. EXPERIMENTAL TEST RESULTS AND DISCUSSIONS

The nano-indentation on the "Vickers microhardness" testers were utilized to investigate the mechanical properties of the welded samples. By carrying out a microhardness test, one may determine the level of the material's power.

4.1 "Vickers Micro Hardness Test" (VMHT)

The Vickers hardness (V.H.) scale utilizes an indenter in the pattern of a diamond that produces a pyramidal indentation on the material surface being evaluated (S. Thirumaran, 2017). The diagonal dimensions of this indentation were measured. The value is used to calculate the V.H. The value of V.H. was determined by dividing the load that was used to make the indentation on the exterior of the samples by the surface area (S.A.) of the indentation. In this investigation, a VMHT with a load of 200 grams and a testing time of 15 secs. was used. These modifications produced an indentation which is sufficiently significant to allow for the extraction of accurate data from the specimens. Using SiC abrasive papers surface of material is polished which is then followed by low speed disc-polishing and the sample is kept flat as long as possible. Indentation studies will produce the best possibilities as a direct result of this.

Vickers Micro Hardness Testing Machine

Specifications of Vickers Micro Hardness Testing Machine are:

- Windows 10-based software for the measurement of indentation is provided
- There is no requirement of P.C. and Antivirus.
- For both normal and overview cameras, dual screens are provided
- Multiple samples can be programmed at a time
- Baby Brinell as well as knop hardness scales, can be performed
- 4, 6 and 8 positions are included depending upon the type of model

Table 3: Vickers Hardness of Materials

Material	Specified Hardness in H.V.	Observed Hardness in H.V.
Stainless Steel	120 – 140 HV	135 HV
EN_3B	120 – 140 HV	135 HV
Mild Steel	120 – 136 HV	130 HV

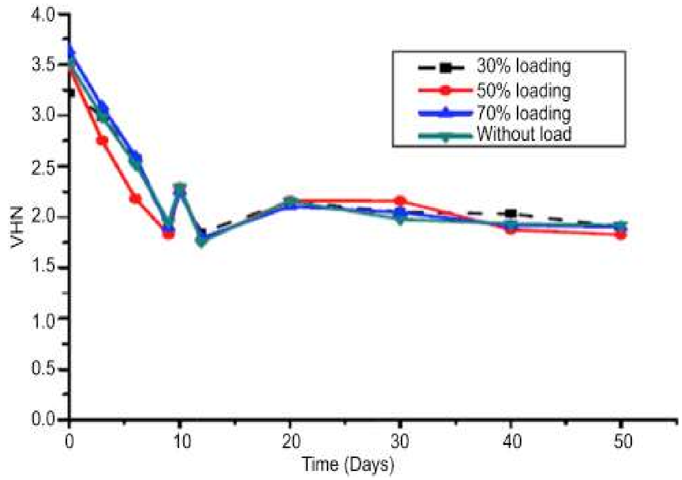

Figure 3: Relationship of Vickers Hardness of Material with time

To test the hardness of welded material, VMHT was applied. The ASTM E384-01 standard was adopted for the hardness readings evaluation, whereas the ASTM E407-01 standard was implemented for the micro tests. In order to conduct the study, a hardness traverse was drawn at a distance of 0.1mm. The values of the hardness were consistent across all of the specimens. The re-crystallization operations occurring at the H.A.Z. cause the reduction in "hardness value" (Mild Steel side). The highest possible hardness value of 450 Hv was measured in the area of the weld joint.

4.2 Traverse Force

When welding, a force known as traverse force acts along the line and is exerted by the pliable material on the tool pin (and the tool itself) as they traverse back and forth. Knowing how this variable impacts the mechanics of material motion during the FSW process is essential. Tool profile, process parameters, B.M. composition (type), and B.M. thickness all have an impact on the required transverse force. The flow stress, which is highly dependent on the temperature of the pliable material, has been shown in the literature to be strongly related to the traverse force. It is well knowledge that as temperature rises, flow stress falls (Outinen, 2007). Previous research on the movement of materials has shown that the coalescence results from the gradual accumulation of layers of sediment around the pin (Attallah et al., 2007). When new layers are being deposited, transverse force is shown to fluctuate at a high frequency but a small amplitude. Some scholars have studied the phenomena of material flow by investigating the work and tool material simultaneously using the abrupt machine-stop approach. They came to the conclusion that coalescence and S.Z. (weld nugget) creation occur because sheared layers of materials are deposited around the tool pin location (Schmidt et al., 2006; Krishnan, 2002). However, the FSW process's sheared layers rotate with the tool pin and get unattached behind the tool pin, a phenomenon that was not explained by the rapid tool stop approach. Materials flow between the faying surfaces of the B.M., and the tool pin was the subject of another investigation, which aimed to characterize the mechanism of this transfer (Lin et al., 2007). They hypothesized that, with the tool pin serving as the journal and the B.M. as the bearing, the material-flow mechanism would be similar to that of a flowing lubricant in a journal

bearing. Similarly to how bearing pressure on journal inside a bearing depends on projected area of the journal, tool rotational speed, and fluid viscosity, Lin et al. (2007) reported that during FSW, the radial stress around the leading side of the pin depends on the material corresponding to the temperature existing at the pin surface. To calculate the traverse force, multiply the yield stress by the predicted area of the tool pin, as shown above. Hence, a higher traverse speed results in a lower weldment
Minitab-17, a widely used statistical analysis program, was used to examine the traverse force data from each experiment. The "lower-the-better" criteria were used for the analysis of traverse force because a low value of traverse force exerts less strain on the work fixture, the machine spindle, and the tool. The ANOM method was used to zero in on the most important influences on each variable and find the sweet spot for tuning. Table B displays the results of experiments measuring traversing forces (Appendix-II). In Table 4.3, we can see the ANOM findings for the traverse force.

Table 4.3: "Response Table for S/N ratio (Traverse force)".

F.S.W. Parameters	Unit	Symbol	Level-1	Level-2	Difference	Rank
Speed of Tool Rotation	Rpm	A	-70.88	-69.45	1.44	1
Traversing speed	mm/min	B	-69.44	-70.69	1.06	2
Shoulder diameter	mm	C	-70.21	-70.12	0.09	3

Table 4.3 demonstrates how the FSW parameters change in response to changes in the traverse force. Both the rotational and linear velocities of the tool are important, but especially A and

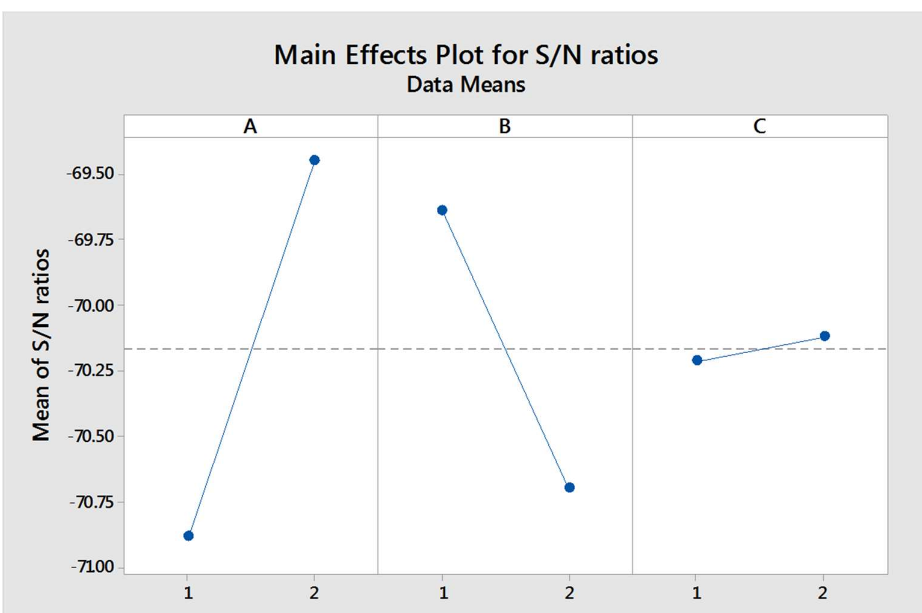

B. Fig.4.9 displays a major effects plot for the S/N ratio, demonstrating the optimum parameter combination for the traverse force.
Fig. 4.9: "Main effect plots" for S/N ratio (Traverse force).

Factors and their interactions that substantially impact the traversal force were identified using analysis of variance. Validation of the assumption of normality of the residuals is necessary for the usage of ANOVA. A normal probability plot was generated in Minitab 17 to check the residuals for a normal distribution (see Fig. 4.10).

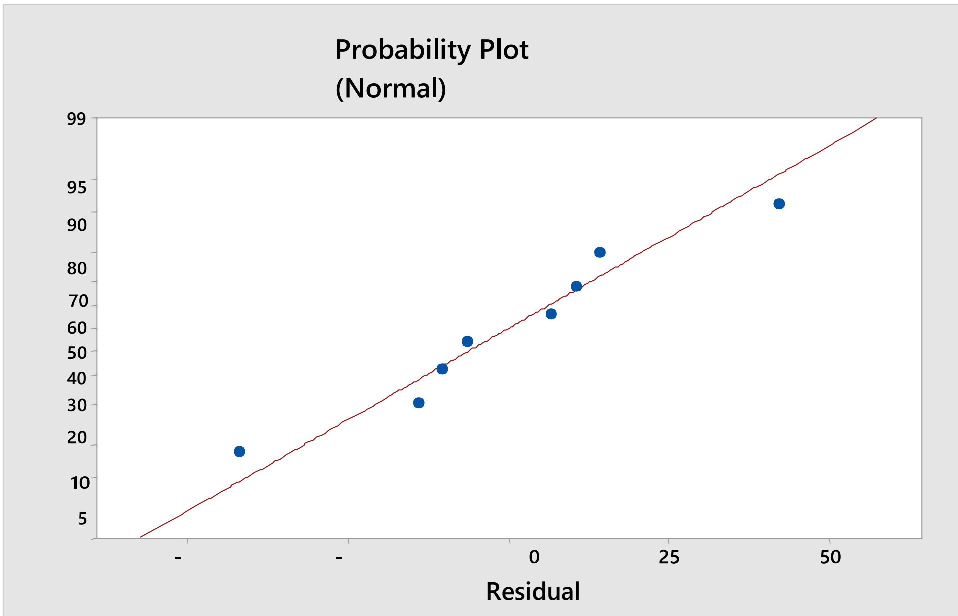

Fig. 4.10: Probability plot (Normal) for S/N ratio (Traverse force).

From Fig. 4.10, we can see that all residual data points lie on or very near the straight line. This confirms that the data are normally distributed, a prerequisite for using ANOVA. Analysis of variance was then used to examine the effect of FSW parameters and their interactions on the traversing force. Statistics for the analysis of variance are shown in Table 4.4. Tool rotational speed and tool traversal speed make up two of the three variables in the fast-short-weird test., substantially impact the traverse force (p-value 0.05), as demonstrated by the ANOVA findings in Table 4.4. The third element, tool shoulder diameter, does not have a major role in the traverse force, however. The traverse force is also heavily influenced by the feedback loop between the tool's rotating speed (A) and the travel speed (B). Other than statistical significance, ANOVA findings also provide the relative importance of each factor and the degree of interaction between them.

Table 4.4: The ANOVA table for Traverse force.

Source	Sum of Squares	DF	Mean Square	F Value	P-value	% Contribution
A	4.119	1	4.119	1119.740	0.019	49.37
B	2.232	1	2.232	606.700	0.026	26.75
C	0.017	1	0.017	4.5700	0.278	0.20
AB	1.969	1	1.969	535.270	0.027	23.60
AC	0.001	1	0.001	0.210	0.728	0.01
BC	0.002	1	0.002	0.550	0.592	0.02
Residual	0.004	1	0.004			
Total	8.343	7				

The significance of each parameter on the response (here, the traverse force) is shown by its percentage contribution. It is found that the most contributor (49.37%) to traversal force is the tool's rotating speed (parameter A). Parameter B, traversal speed, is likewise a significant contribution to the traversal force, making up 26.75 percent of the total. The third component, tool shoulder diameter (parameter C), contributes hardly little at 0.20%. Counting down from the most significant to the least significant, the contributions of interactions (A.B.) (23.6%), (B.C.) (0.02%), and (A.C.) (0.01%) can be shown.
Traverse forces were found to be minimal when the tool rotational speed was 560 rpm, the traverse speed was 40 mm/min, and the shoulder diameter was 14 mm, as shown in Table 4.4 and Table 4.3, respectively.

Also, a regression analysis was run to establish the link between FSW parameters and traversal force. The equation for the predicted traversal force, in terms of the known FSW parameters and their interactions, is given by (4.2).

$Traverse\ force avg = 1670 + 615.2A + 1681.8B - 24.8C - 806AB + 24.1AC - 32BC$
(4.2)
The value of the coefficient of determination, R2 for short, defines the importance of the connection between the traverse force and the current parameters. A high R-squared value (99.94%) is found for Eqn. (4.2), showing that almost all of the variation in the value of traversal force can be accounted for by changes in the FSW parameters (0.06%). Therefore, this indicates that there is a robust link between traverse force and FSW parameters and that it may be utilized to forecast the precise values of traverse force for varied values of FSW parameters. The following sections detail how changing the FSW settings affects the traversal force:

5. CONCLUSION & FUTURE SCOPE

In order to join two different types of steel together, friction welding has been used. Overall, the produced joints showed high strength and a fair amount of ductility. When it comes to deciding the qualities of the weld, the CC of the steels that are applied in the welding process plays a significant importance. During the F.W. process, the metal has a tendency to shorten in length and will exhibit a flash formation when it does so. The weld zone does not have a hardness value when micro hardness is measured in welded material. There is no weld zone because of the sticky layer on the joint. With large production, consolidated welding proved to be more efficient and generate more productivity with lower costs.

Aside from general corrosion research findings, more research can be done on how prone something is to cold cracking and what microstructural features are important for cracking. The method of F.W. can also be used on plastics that harden when heated.

REFERENCES

1. Afolalu, Adeniran & Ohwofa, A & Ongbali, Samson & Ajayi, O & Abioye, Abiodun. (2019). Microstructural and Mechanical Properties of Welded Joints in Tig, Mig and Friction Stir Welding –Review. *IOP Conference Series: Materials Science and Engineering*. *640*.
2. B. Srinivas, N. K. (2018). Studies on post weld heat treatment of dissimilar aluminum alloys by laser beam welding technique. *I.O.P. Conference Series Materials Science and Engineering, 330*(1).
3. Fehim Findik, R. Y. (2011). he effects of heat treatment on the microstructure and microhardness of explosive welding. *Scientific Research and Essays*, 4141-4151
4. P. ShenbagaVelu, N. Rajesh Jesudoss Hynes (2016), Numerical analysis of friction welded titanium joints, JAMME, PP:26-29.
5. R. Palanivel (2016),An investigation into the effect of friction welding parameters on tensile strength of titanium tubes by utilizing an empirical relationship, Measurement, MEASUR 4456,Pp 1-45.
6. Takeshi Shinoda (1994), Effect of Friction Welding Parameters on Mechanical Properties of Cast Iron Joints, Journal of Japan Welding Society, Vol. 12, No. 3, pp :328-334.
7. S. PandiaRajan et al (2016) ,An investigation on SA 213 tube to SA 387 tube plate with backing block arrangement in friction welding process, Alexandria Engineering Journal, No 55, pp:1255–1269.
8. M. Kimuraa et al (2017),Effect of friction welding condition on joining phenomena: tensile strength and bend ductility of friction welded joint between pure aluminum and AISI 304 stainless steel, Journal of Manufacturing Processes No:25,pp:116–125.
9. Z. Liang et al (2015),Microstructural characterization and mechanical properties of dissimilar friction welding of 1060 aluminum to AZ31B magnesium alloy, MSA32627,pp 1-26.
10.

11. G. Ananda Rao, B. R. (2021). Study the effect process of parameters on friction welding of dissimilar metals AISI 304 steel and AA 2219 aluminium., *2317*.

12. H. T. Hsieh, J. L. (2009). Using TRIZ methods in friction stir welding design. *The International Journal of Advanced Manufacturing Technology, 46*(9), 1085-1102.

13. Kimura, M., K. Suzuki, M. Kusaka, and K. Kaizu. 2017. "Effect of Friction Welding Condition on Joining Phenomena, Tensile Strength, and Bend Ductility of Friction Welded Joint between Pure Aluminium and AISI 304 Stainless Steel." *Journal of Manufacturing Processes* 25: 116–25.

14. Sahin, Mümin. (2005). Joining with Friction Welding of High-Speed Steel and Medium-Carbon Steel. *Journal of Materials Processing Technology* 168(2): 202–10. https://linkinghub.elsevier.com/retrieve/pii/S0924013604013123.

15. Sahin, M. (2009), "Joining of stainless steel and copper materials with friction welding", *Industrial Lubrication and Tribology*, Vol. 61 No. 6, pp. 319-324. https://doi.org/10.1108/00368790910988435